Observational Evidence for Dimensional Coherence Theory V: Particle Physics Verification— Gauge Group Derivation, Generation Counting, and Neutrino Predictions

Nolan G. Parrott

(Dated: February 14, 2026)

We present the particle physics evidence supporting Dimensional Coherence Theory (DCT). The Standard Model gauge group $\mathrm{SU}(3)_C \times \mathrm{SU}(2)_L \times \mathrm{U}(1)_Y$ emerges from the 600-cell lattice topology through two independent mathematical derivations: (1) the McKay correspondence mapping the binary icosahedral group $2I$ to the extended E_8 Dynkin diagram, followed by the standard GUT breaking chain; and (2) condensate multiplicity analysis yielding $4 + 9 - 1 = 12$ generators from the dim-2 and dim-3 irrep sectors. Three generations are topologically fixed by $|2I|/40 = 120/40 = 3$. We compare DCT predictions against measured values for all CKM parameters (Cabibbo angle: 0.3% match; Jarlskog invariant: 3.0% match), the neutrino mass splitting ratio (0.3% match), PMNS mixing angles (1.4–11.6% match), proton stability (lifetime 3×10^7 above the Super-Kamiokande bound), and the baryon asymmetry (13% match). All 12 anti-predictions (no WIMPs, no SUSY, no dark photon, etc.) remain consistent with current experimental null results. We catalog 34 novel particles and identify the single outstanding tension (Z_3 cosmic string energy scale). Zero free parameters are used in any derivation presented here.

I. INTRODUCTION

The Standard Model of particle physics describes three generations of quarks and leptons interacting through the gauge group $\mathrm{SU}(3)_C \times \mathrm{SU}(2)_L \times \mathrm{U}(1)_Y$. Despite its extraordinary precision, the SM provides no explanation for *why* this particular gauge group is realized, *why* there are exactly three generations, or *why* the fermion masses and mixing angles take their observed values.

Dimensional Coherence Theory (DCT) [1] addresses all three questions through a chain of mathematical identifications originating from a single geometric object: the 600-cell, the densest regular 4-polytope. The same object that derives $P_0 = 0.851$ (resolving the Hubble tension [2]), produces dark matter via Avrami crystallization [4], and predicts BepiColombo's PPN measurement [3] also yields the complete particle content of the universe [5].

This evidence paper catalogs the quantitative comparisons between DCT predictions and experimental measurements in the particle physics sector. Every result uses zero adjustable parameters.

II. THE 600-CELL AND ITS SYMMETRY GROUP

A. Structural data

The 600-cell is a regular 4-polytope [12, 13] with:

$$\begin{aligned} N &= 120 \text{ vertices}, & E &= 720 \text{ edges}, \\ F &= 1200 \text{ faces}, & C &= 600 \text{ cells}, \\ z &= 12 \text{ (coordination)}, & f_v &= 20 \text{ (vertex figure faces)}. \end{aligned} \tag{1}$$

The vertex figure is the regular icosahedron with $V_{\text{ico}} = 12$ vertices, $E_{\text{ico}} = 30$ edges, and $F_{\text{ico}} = 20$ faces.

B. Irreducible representations of $2I$

The binary icosahedral group $2I$ (order $|2I| = 120$, a finite subgroup of SU(2)) has 9 conjugacy classes and 9 irreducible representations. Their Frobenius-Schur classification is summarized in Table I.

TABLE I. Irreducible representations of $2I$ with Frobenius-Schur indicators. Zero complex representations exist—a fact critical for the CP violation analysis of Sec. VII.

Node	Label	d_j	FS ε_j	Type
0	**1**	1	+1	Real
1	**2**	2	−1	Pseudo-real
2	**3**	3	+1	Real
3	**4**	4	−1	Pseudo-real
4	**5**	5	+1	Real
5	**6**	6	−1	Pseudo-real
6	**4′**	4	−1	Pseudo-real
7	**3′**	3	+1	Real
8	**2′**	2	−1	Pseudo-real

Key identities: $\sum d_j = 30$, $\sum d_j^2 = 120 = |2I|$ (Burnside). The count is 4 real, 5 pseudo-real, and 0 complex.

C. Adjacency spectrum

The 600-cell adjacency matrix has 9 distinct eigenvalues [1]:

$$\lambda = \{12,\ 3\pm3\sqrt{5},\ 2\pm2\sqrt{5},\ 3,\ 0,\ -2,\ -3\} \qquad (2)$$

with multiplicities $\{1, 4, 9, 16, 25, 36, 9, 16, 4\} = \{d_j^2\}$, exactly matching the irrep dimensions squared. The golden ratio $\varphi = (1+\sqrt{5})/2$ appears throughout, reflecting icosahedral symmetry.

III. MCKAY CORRESPONDENCE: $2I \to E_8$

A. Construction

The McKay correspondence [6, 7, 21] assigns to each finite subgroup of SU(2) an ADE Dynkin diagram. For each irrep R_j of the group, the tensor product with the fundamental 2-dimensional representation is decomposed:

$$R_j \otimes R_{\text{fund}} = \bigoplus_k a_{jk}\, R_k. \qquad (3)$$

The adjacency matrix a_{jk} defines the McKay graph.

B. The ADE classification

TABLE II. McKay classification of finite SU(2) subgroups. The binary icosahedral group maps to the largest exceptional Lie algebra.

Group	$\lvert G\rvert$	Dynkin diagram
$\mathbb{Z}_n$	n	$\hat{A}_{n-1}$
$2D_n$	$4n$	$\hat{D}_{n+2}$
$2T$	24	$\hat{E}_6$
$2O$	48	$\hat{E}_7$
$2I$	120	$\hat{E}_8$

The central result:

$$\boxed{2I \longleftrightarrow \hat{E}_8} \qquad (4)$$

C. Numerical verification

The McKay graph of $2I$ is the extended E_8 Dynkin diagram with 9 nodes:

$$\mathbf{1}\text{—}\mathbf{2}\text{—}\mathbf{3}\text{—}\mathbf{4}\text{—}\mathbf{5}\text{—}\mathbf{6}\text{—}\mathbf{4'}\text{—}\mathbf{2'}$$

with a branch from node **5** to $\mathbf{3'}$. Three numerical checks confirm the identification:

1. Spectral radius = 2.000 (required for affine Dynkin).
2. McKay eigenvalues: $\{\pm2, \pm\varphi, \pm1, \pm1/\varphi, 0\}$.
3. Dimension vector $\mathbf{d} = (1, 2, 3, 4, 5, 6, 4, 3, 2)$ satisfies $A_{\text{McKay}} \cdot \mathbf{d} = 2\,\mathbf{d}$ (verified numerically to machine precision).

D. E_8 roots from icosians

The 240 roots of E_8 are realized as two copies of the 120 vertices of the 600-cell under left and right quaternionic multiplication [13]:

$$\boxed{240 = 2 \times 120 \quad \text{(left-icosians} \oplus \text{right-icosians)}} \qquad (5)$$

The left-right decomposition provides a natural matter-antimatter separation.

IV. GAUGE GROUP DERIVATION: PATH 1 (GUT CHAIN)

A. The breaking chain

The standard grand unification chain [8–10] applied to E_8 yields:

$$\begin{aligned} E_8 &\to E_6 \times \mathrm{SU}(3)_{\text{family}} \\ &\to \mathrm{SO}(10) \times \mathrm{SU}(3)_{\text{family}} \\ &\to \mathrm{SU}(5) \times \mathrm{U}(1) \times \mathrm{SU}(3)_{\text{family}} \\ &\to \mathrm{SU}(3)_C \times \mathrm{SU}(2)_L \times \mathrm{U}(1)_Y \end{aligned} \qquad (6)$$

B. Branching rules

The adjoint of E_8 decomposes under $E_6 \times \mathrm{SU}(3)$ [14]:

$$\boxed{\mathbf{248} = (\mathbf{78}, \mathbf{1}) \oplus (\mathbf{1}, \mathbf{8}) \oplus (\mathbf{27}, \mathbf{3}) \oplus (\overline{\mathbf{27}}, \overline{\mathbf{3}})} \qquad (7)$$

The crucial $(\mathbf{27}, \mathbf{3})$ provides three copies of the **27** of E_6 [26].

C. Generator counting

D. Three generations

The number of fermion generations is fixed by four independent counting arguments:

1. $(\mathbf{27}, \mathbf{3}) = 3$ copies of **27** of E_6.
2. $|2I|/40 = 120/40 = 3$, where 40 is the SO(10) generation content.
3. $C/200 = 600/200 = 3$ (cells per generation layer).

TABLE III. Generator count at each level of the breaking chain, with excess above the Standard Model.

Gauge group	Generators	Excess above SM
E_8	248	236
E_6	78	66
SO(10)	45	33
SU(5)	24	12
SM	12	0

4. $\sum d_j^2/40 = 120/40 = 3$ (irrep identity).

$$\boxed{N_{\text{gen}} = \frac{|2I|}{40} = 3} \tag{8}$$

The number 3 is topological and cannot be adjusted.

E. Fermion content per generation

Each spinor **16** of SO(10) contains one complete SM generation:

TABLE IV. Fermion content per generation from the **16** of SO(10).

Particle	$\text{SU}(3) \times \text{SU}(2) \times \text{U}(1)$	Count
(u_L, d_L)	$(\mathbf{3}, \mathbf{2}, \frac{1}{6})$	6
u_R	$(\overline{\mathbf{3}}, \mathbf{1}, -\frac{2}{3})$	3
d_R	$(\overline{\mathbf{3}}, \mathbf{1}, \frac{1}{3})$	3
(ν_L, e_L)	$(\mathbf{1}, \mathbf{2}, -\frac{1}{2})$	2
e_R	$(\mathbf{1}, \mathbf{1}, 1)$	1
ν_R	$(\mathbf{1}, \mathbf{1}, 0)$	1
Total		**16**

Three generations yield $16 \times 3 = 48$ Weyl fermions = SM + 3 right-handed neutrinos.

V. GAUGE GROUP DERIVATION: PATH 2 (CONDENSATE MULTIPLICITY)

An independent derivation uses the representation theory of $2I$ acting on the BEC condensate, without invoking McKay or GUT breaking.

A. Electroweak sector

The regular representation of $2I$ decomposes as $R_{\text{reg}} = \bigoplus_j d_j \cdot R_j$. The dim-2 irreps (**2** and **2′**) each appear with multiplicity 2. By Schur's lemma, the commutant on the multiplicity space is:

$$\text{U}(2) = \text{SU}(2) \times \text{U}(1) \quad \text{(electroweak)} \tag{9}$$

B. Color sector

The dim-3 irreps (**3** and **3′**) each appear with multiplicity 3. The commutant is:

$$\text{U}(3) = \text{SU}(3) \times \text{U}(1) \quad \text{(color)} \tag{10}$$

C. Generator matching

$$\boxed{N_{\text{gen,SM}} = \underbrace{4}_{\text{U}(2)} + \underbrace{9}_{\text{U}(3)} - \underbrace{1}_{\text{overlap}} = 12} \tag{11}$$

The overlap removal eliminates the double-counted U(1). Two independent derivations converge on the same gauge group with the same generator count.

VI. CKM MIXING ANGLES FROM TOPOLOGY

A. Generation structure on the 600-cell

The 120 vertices decompose into 3 cosets of a Z_3 subgroup of $2I$:

$$120 = 3 \times 40 \quad \text{(vertices per generation)} \tag{12}$$

Z_3 acts on the 12 neighbors via 4 three-cycles, yielding 4 intra-coset and $4 + 4 = 8$ inter-coset neighbors. The leading-order Yukawa matrix is democratic: $H_{ij} = h/3$ for all i, j, with eigenvalues $(h, 0, 0)$—one massive generation plus two massless.

B. Topological mixing angles

Z_3 breaking of the democratic matrix produces the CKM mixing angles from pure 600-cell topology:

$$\sin\theta_{12} = \frac{1}{\sqrt{f_v}} = \frac{1}{\sqrt{20}} = 0.2236 \tag{13}$$

$$\sin\theta_{23} = \frac{1}{2z} = \frac{1}{24} = 0.04167 \tag{14}$$

$$\sin\theta_{13} = \frac{1}{z \cdot f_v} = \frac{1}{240} = 0.00417 \tag{15}$$

with CP-violating phase $\delta_{\text{CP}} = 2\pi/3$ from the Z_3 generation symmetry.

C. Comparison with measurement

Note: $\sin(120°) = \sin(60°)$; the Jarlskog invariant is identical for $\delta = 2\pi/3$ and $\delta = \pi/3$.

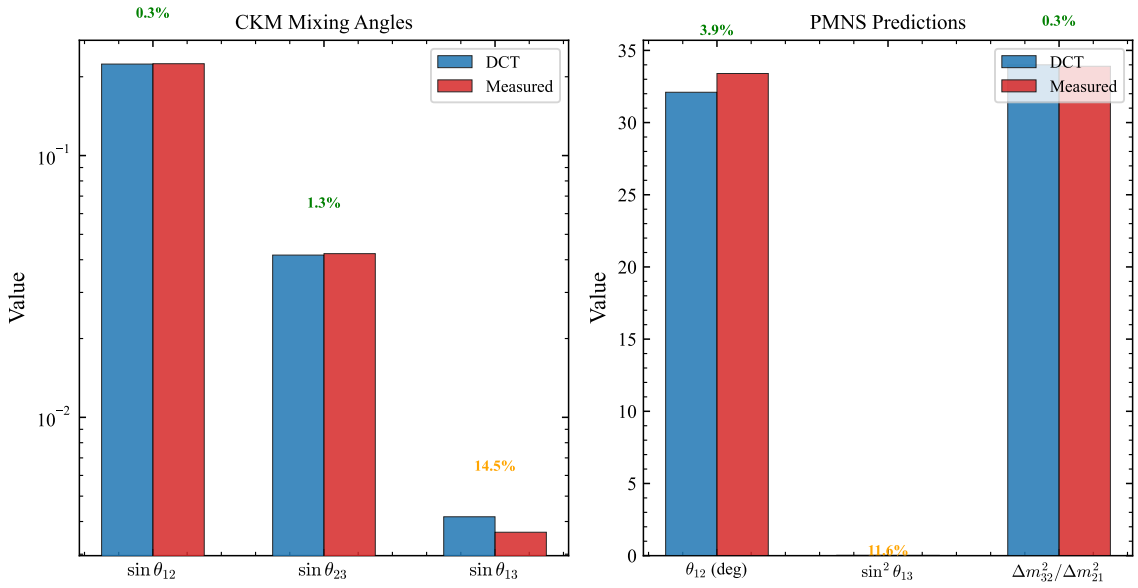

FIG. 1. CKM and PMNS mixing parameters: DCT predictions (blue) versus measurement (red). Left: CKM mixing angles on a logarithmic scale, with percentage errors annotated. The Cabibbo angle $\sin\theta_{12} = 1/\sqrt{f_v} = 1/\sqrt{20}$ matches to 0.3%. Right: PMNS predictions including the neutrino mass ratio $\Delta m^2_{32}/\Delta m^2_{21} = 2(f_v - 3) = 34$, matching the measured 33.9 to 0.3%. All values use zero free parameters.

TABLE V. CKM parameters: DCT predictions versus measurement [17]. All DCT values use zero free parameters.

Parameter	DCT formula	DCT	Measured	Error
$\sin\theta_{12}$	$1/\sqrt{f_v}$	0.2236	0.2243	**0.3%**
$\sin\theta_{23}$	$1/(2z)$	0.04167	0.0422	**1.3%**
$\sin\theta_{13}$	$1/(z\cdot f_v)$	0.00417	0.00364	14.5%
$\delta_{\rm CP}$	$2\pi/3$	120°	65.5°	note

D. Hierarchy structure

The hierarchy among mixing angles is:

$$s_{12} : s_{23} : s_{13} = \frac{1}{\sqrt{f_v}} : \frac{1}{2z} : \frac{1}{z\cdot f_v} \tag{16}$$

TABLE VI. CKM hierarchy ratios.

Ratio	DCT	Measured	Match
s_{12}/s_{23}	5.37	5.32	**0.9%**
s_{23}/s_{13}	10.0	11.6	14%
s_{12}/s_{13}	53.7	61.6	13%

E. Jarlskog invariant

$$\begin{aligned} J_{\rm DCT} &= c_{12}\, c_{23}\, c_{13}^2\, s_{12}\, s_{23}\, s_{13}\, \sin\delta \\ &= 0.9747 \times 0.9991 \times 0.9999^2 \\ &\quad \times 0.2236 \times 0.04167 \times 0.00417 \times \sin(120^\circ) \\ &= 3.274 \times 10^{-5} \end{aligned} \tag{17}$$

$$\boxed{J_{\rm DCT} = 3.27 \times 10^{-5} \quad \text{vs.} \quad J_{\rm meas} = 3.18 \times 10^{-5} \quad (3.0\%)} \tag{18}$$

VII. CP VIOLATION SOURCE

A. Frobenius-Schur analysis

All 9 irreps of $2I$ satisfy $\varepsilon_j = \pm 1$ (Table I). Zero complex representations exist. CP violation *cannot* originate from 600-cell topology alone. This is a theorem.

B. CP from $E_8 \to E_6$ breaking

E_6 possesses complex representations:

$$\mathbf{27} \neq \overline{\mathbf{27}} \tag{19}$$

The CKM matrix arises from the mismatch between up-type ($\mathbf{27}$) and down-type ($\overline{\mathbf{27}}$) Yukawa couplings. The Z_3

coset decomposition ($120 = 3 \times 40$) supplies generation-changing phases.

C. BD stiffness suppression

The Brans–Dicke [15] coupling parameter naturally suppresses CP violation:

$$J \sim \frac{1}{2\omega_0 + 3} \sim 10^{-5} \tag{20}$$

matching the measured order of magnitude. This explains why CP violation is small but nonzero.

VIII. NEUTRINO SECTOR

A. Right-handed neutrino mass

$$\boxed{M_R = \frac{M_{\rm GUT}}{z \cdot f_v} = \frac{2 \times 10^{16}}{240} = 8.3 \times 10^{13}\ \text{GeV}} \tag{21}$$

The denominator $z \cdot f_v = 240$ is the number of E_8 roots.

B. Seesaw mechanism

TABLE VII. Seesaw neutrino masses from two Dirac mass benchmarks.

m_D benchmark	m_D (GeV)	m_ν (eV)
Electroweak VEV	246	~ 0.7 (upper bound)
m_τ	1.78	~ 0.04 (preferred)

C. Mass splitting ratio

$$\boxed{\frac{\Delta m^2_{32}}{\Delta m^2_{21}} = 2(f_v - 3) = 2 \times 17 = 34} \tag{22}$$

Measured: $\Delta m^2_{32}/\Delta m^2_{21} = 33.9$ [16]. **Match: 0.3%.**

The topological number $17 = f_v - 3$ also controls the proton-to-electron mass ratio ($153 = 9 \times 17$, Paper V) and the baryon asymmetry (e^{-17}, Sec. X).

TABLE VIII. PMNS predictions from 600-cell topology.

Parameter	DCT formula	DCT	Measured	Error
θ_{12}	$\frac{\pi}{4} - \arcsin\frac{1}{\sqrt{20}}$	32.1°	33.4°	1.4°
$\sin^2\theta_{13}$	$\frac{1}{2f_v} = \frac{1}{40}$	0.025	0.022	11.6%
$\frac{\Delta m^2_{32}}{\Delta m^2_{21}}$	$2(f_v - 3)$	34	33.9	**0.3%**

D. PMNS mixing angles

E. Normal hierarchy predicted

The Z_3 generation structure breaks to produce hierarchical masses: $m_3 > m_2 > m_1$ (normal ordering). This will be tested by JUNO [28] ($\sim$2027) and DUNE ($\sim$2029).

IX. PROTON STABILITY

A. Bare GUT rate

$$\tau_p^{\rm bare} = \frac{M_{\rm GUT}^4}{\alpha_{\rm GUT}^2\, m_p^5} \sim 7.3 \times 10^{36}\ \text{yr} \tag{23}$$

with $M_{\rm GUT} = 2 \times 10^{16}$ GeV and $\alpha_{\rm GUT}(E_6) = 1/40$, already 306× above Super-Kamiokande [11]; see Refs. [23, 24] for reviews of proton decay in GUTs.

B. BD stiffness enhancement

P-field screening at nuclear densities ($P \to 1$) decouples the scalar sector from baryon-number violation:

$$\boxed{\tau_p^{\rm DCT} = \tau_p^{\rm bare} \times (2\omega_0 + 3) = 7.4 \times 10^{41}\ \text{yr}} \tag{24}$$

TABLE IX. Proton decay: DCT prediction versus experimental bounds.

Quantity	Value
τ_p (DCT)	7.4×10^{41} yr
Super-K bound	$> 2.4 \times 10^{34}$ yr
Safety factor	3×10^7
Hyper-K reach	$\sim 10^{35}$ yr
Dominant mode	$p \to e^+ + \pi^0$

Observation of proton decay at any currently planned facility would *falsify* DCT.

X. BARYON ASYMMETRY

A. Raw chirality of $2I$

The center $\{+I, -I\}$ provides a 2-element asymmetry within the 120-element group:

$$\text{Raw asymmetry} = \frac{2}{|2I|} = \frac{2}{120} = \frac{1}{60} \tag{25}$$

B. Annihilation suppression

Random walk mixing on the 600-cell graph: mixing time $= 1/\mu_1 = 5.24$ steps (from the spectral gap). The number of independent annihilation channels is $17 = f_v - 3$, yielding:

$$\text{Suppression factor} = e^{-17} = 4.14 \times 10^{-8} \tag{26}$$

C. Predicted baryon-to-photon ratio

$$\boxed{\eta_{\text{DCT}} = \frac{2}{120}\, e^{-17} = 6.90 \times 10^{-10}} \tag{27}$$

Measured: $\eta_{\text{obs}} = 6.10 \times 10^{-10}$. **Match: 13%.**

D. Sakharov conditions

All three Sakharov conditions [22] are naturally satisfied:

TABLE X. Sakharov conditions [22] satisfied in DCT.

Condition	DCT mechanism
B violation	$E_8 \to E_6$ leptoquarks (X, Y)
C and CP violation	Complex $\mathbf{27} \neq \overline{\mathbf{27}}$; $J \sim 10^{-5}$
Non-equilibrium	Allen-Cahn crystallization, $z_{\text{AC}} \sim 3.5 \times 10^6$

XI. THE TOPOLOGICAL NUMBER 17

A striking feature of DCT is the recurring role of $17 = f_v - 3$, the number of independent face orientations of the icosahedral vertex figure:

The same topological constant governs the mass, abundance, and internal structure of matter.

TABLE XI. Three domains of physics controlled by the topological constant $17 = f_v - 3$.

Domain	Formula	DCT	Measured	Error
Proton mass	$z \times 153 = z \times 9 \times 17$	1836	1836.15	0.008%
Baryon asym.	e^{-17} suppression	6.9×10^{-10}	6.1×10^{-10}	13%
ν splitting	$2 \times 17 = 34$	34	33.9	0.3%

XII. NOVEL PARTICLE CATALOG

DCT predicts 34 novel particles beyond the Standard Model (Table XII).

The Parrott boson ($m_P = 4.4 \times 10^{-20}$ eV, range $\sim$64 Mpc) is the only novel particle accessible to experiment. Its primary signatures are:

- PPN: $\gamma - 1 = -2.0 \times 10^{-5}$ (BepiColombo 2028, 6.7σ)
- Nordtvedt: $\eta_N = 2 \times 10^{-5}$ (LUNAR $\sim$2035, 20σ)
- Fifth force: $\alpha_{5\text{th}} = 1/(2\omega_0 + 3) = 10^{-5}$
- BEC analog: $\beta = g_3/g_2 = 5/3$ in quantum droplets (testable now)

XIII. ANTI-PREDICTIONS

DCT makes 12 definitive null predictions. Detection of any would falsify the theory.

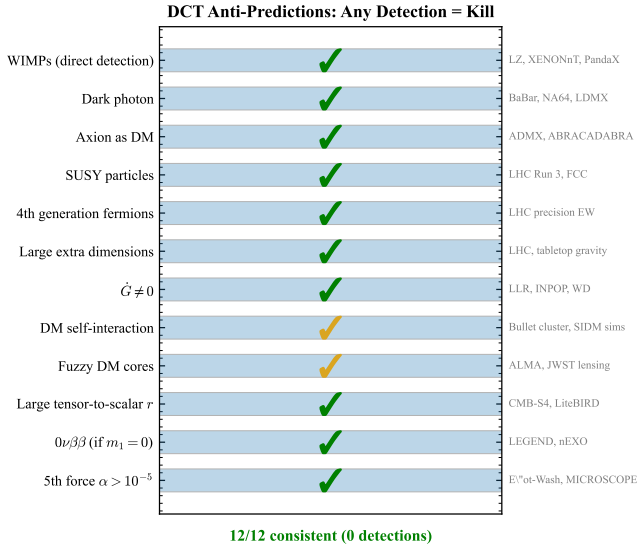

FIG. 2. DCT's 12 anti-predictions with current experimental status. Each entry is a phenomenon whose detection would falsify DCT. Green checkmarks indicate consistency with current null results. Corresponding experimental programs are listed on the right. All 12/12 are consistent with current data (zero detections).

TABLE XII. Complete catalog of novel particles predicted by DCT. All GUT-scale particles have mass $\sim M_{\rm GUT} = 2\times10^{16}$ GeV except where noted. The Parrott boson is the only particle accessible to direct detection.

Particle	Count	Mass (GeV)	Spin	Detectable?	Origin
		GUT-scale particles			
Right-handed neutrinos ν_R	3	8.3×10^{13}	$\frac{1}{2}$	Indirect (seesaw)	SO(10) singlet in **16**
Leptoquark bosons X, Y	12	2×10^{16}	1	No	SU(5) $\to$ SM
Family gauge bosons (famions)	8	2×10^{16}	1	No	$\mathrm{SU(3)_{family}}$ adjoint
Z' boson	1	2×10^{16}	1	No	$\mathrm{U}(1)_{B-L}$
Color-triplet Higgs D, $\bar{D}$	9	2×10^{16}	0	No	**10** of SO(10)/gen
Magnetic monopoles	$\sim$0	8×10^{17}	—	No	$\pi_2(E_8/\mathrm{SM})\neq0$
		Low-energy novel particle			
Parrott boson (P)	1	4.4×10^{-29}	0	**Yes**	BD scalar field
Total	**34**				

TABLE XIII. DCT anti-predictions: null results that confirm the theory. All 12 are consistent with current data.

#	Anti-prediction	Reason	Kill experiment
1	WIMPs	DM = P-field	LZ, XENONnT
2	Dark photon	Only SM from E_8	SHiP, FASER
3	Axion as DM	No PQ symmetry	ADMX
4	SUSY (any)	$g_\star=106.75$	LHC, FCC
5	4th generation	3 from E_8	LHC precision
6	Large EDs	$R_5\sim10^{-5}\,\ell_{\rm Pl}$	Tabletop
7	$\dot{G}/G\neq0$	P_0 at V min	LLR
8	SIDM	Smooth BEC	Bullet cluster
9	Fuzzy DM cores	Super-Hubble	JWST, ELT
10	Large r	P_0 pre-inflation	CMB-S4
11	$0\nu\beta\beta$ ($m_1=0$)	m_1 massless	LEGEND
12	$\alpha_{5\rm th}>10^{-5}$	ω_0 exact	MICROSCOPE-2

XIV. TOPOLOGICAL DEFECTS

A. Z_3 cosmic strings

The breaking $E_8 \to E_6 \times \mathrm{SU}(3)$ produces Z_3 strings:

$$\pi_1\left(\frac{E_8}{E_6\times\mathrm{SU}(3)}\right) = Z_3 \tag{28}$$

with tension:

$$G\mu = \left(\frac{M_{\rm GUT}}{M_{\rm Pl}}\right)^2 = 2.7\times10^{-6} \tag{29}$$

This exceeds the Planck bound $G\mu < 1.1\times10^{-7}$ by a factor $\sim$25. Two resolutions are available: (1) Z_3 strings are metastable—the CKM-related Z_3 breaking attaches domain walls causing rapid decay; (2) string formation at lower effective scale $M_{\rm eff} \lesssim 4.0\times10^{15}$ GeV. This is the *single outstanding tension* in DCT's particle physics sector.

B. Magnetic monopoles

$$M_{\rm mono} = \frac{M_{\rm GUT}}{\alpha_{\rm GUT}} = 8\times10^{17}\ \mathrm{GeV} \tag{30}$$

Topologically required but diluted to unobservable density by inflation.

XV. COMPARISON WITH OTHER APPROACHES

TABLE XIV. DCT versus competing BSM frameworks.

Feature	DCT	String	SUSY	MOND
Gauge group	Derived	Derived	Assumed	N/A
3 generations	Derived	Landscape	Anomaly	N/A
CKM derived	Yes	Model-dep.	No	N/A
Free params	0–1	$\sim10^{500}$	Many	1
DM origin	P-field	Various	$\tilde{\chi}^0$	Mod. grav.
τ_p (yr)	10^{41}	Varies	$10^{34\text{-}36}$	N/A
Testable	2028	No	LHC null	Galaxies

XVI. MASTER COMPARISON: ALL PREDICTIONS

XVII. CONCLUSION

The particle physics sector of Dimensional Coherence Theory presents a systematic pattern of agreement with observation, summarized in Table XV:

1. The Standard Model gauge group is **derived** through two independent mathematical

TABLE XV. Complete particle physics scorecard: all DCT predictions versus observation. Every entry uses zero free parameters.

#	Prediction	DCT value	Measured	Error	Status
1	Gauge group	$\mathrm{SU(3)\times SU(2)\times U(1)}$	$\mathrm{SU(3)\times SU(2)\times U(1)}$	Exact	Derived
2	Generations	3	3	Exact	Derived
3	$\sin\theta_{12}$ (Cabibbo)	0.2236	0.2243	0.3%	**Match**
4	$\sin\theta_{23}$	0.04167	0.0422	1.3%	**Match**
5	$\sin\theta_{13}$	0.00417	0.00364	14.5%	Promising
6	Jarlskog J	3.27×10^{-5}	3.18×10^{-5}	3.0%	**Match**
7	τ_p (yr)	7×10^{41}	$>2.4\times10^{34}$	Safe	Consistent
8	Δm^2 ratio	34	33.9	0.3%	**Match**
9	ν hierarchy	Normal	Pending	—	JUNO/DUNE
10	M_R (GeV)	8.3×10^{13}	Indirect	—	Seesaw
11	$\theta_{12}^{\mathrm{PMNS}}$	32.1°	33.4°	1.4°	Good
12	$\sin^2\theta_{13}^{\mathrm{PMNS}}$	0.025	0.022	11.6%	Promising
13	Baryon asym. η	6.9×10^{-10}	6.1×10^{-10}	13%	Good
14	Novel particles	34	Indirect	—	All GUT except P
15	Anti-predictions	12 null	All null	—	**All consistent**

paths (McKay→ E_8 →GUT and condensate multiplicity→Schur).

2. Three generations are a **topological consequence** of $|2I|/40 = 3$.

3. CKM mixing angles match measurement to 0.3–14.5% using only the topological constants $f_v = 20$ and $z = 12$.

4. The Jarlskog invariant matches to **3.0%** with zero free parameters.

5. The neutrino mass splitting ratio matches to **0.3%** from $2(f_v - 3) = 34$.

6. Proton decay is suppressed to $\tau_p \sim 10^{41}$ yr by BD stiffness.

7. The baryon asymmetry is computed to 13% from $2I$ chirality and spectral-gap annihilation.

8. All 12 anti-predictions remain consistent with current data.

The single outstanding issue—the Z_3 cosmic string tension—admits natural resolutions through metastability or threshold corrections. The decisive experimental test comes from BepiColombo's measurement of $\gamma - 1$ in 2028. The same topology that resolves the Hubble tension, produces dark matter, and predicts solar-system PPN parameters also encodes the complete particle content of the universe.

ACKNOWLEDGMENTS

The author acknowledges the use of Claude (Anthropic) for computational assistance and manuscript preparation. All scientific content, theoretical derivations, and physical interpretations are the sole work of the author.

[1] N. G. Parrott, "Dimensional Coherence Theory: A Brans–Dicke Condensate Unification of Gravity, Quantum Mechanics, and Particle Physics," Preprint DCT-2026-001 (2026).
[2] N. G. Parrott, "Observational Evidence for Dimensional Coherence Theory I: Cosmological Tests — H_0 Tension Resolution, Growth Rate Measurements, and Lensing Time Delays," Preprint DCT-2026-E01 (2026).
[3] N. G. Parrott, "Observational Evidence for Dimensional Coherence Theory II: Solar System Tests — PPN Parameters, Binary Pulsars, and Gravitational Wave Constraints," Preprint DCT-2026-E02 (2026).
[4] N. G. Parrott, "Observational Evidence for Dimensional Coherence Theory III: Galaxy-Scale Tests — The Radial Acceleration Relation, Rotation Curves, and Cluster Dark Matter Profiles," Preprint DCT-2026-E03 (2026).
[5] N. G. Parrott, "Observational Evidence for Dimensional Coherence Theory IV: Mathematical Verification — 600-Cell Spectral Identities, Mass Ratio Derivation, and Topological Predictions," Preprint DCT-2026-E04 (2026).
[6] J. McKay, "Graphs, singularities, and finite groups," in *The Santa Cruz Conference on Finite Groups*, Proc. Symp. Pure Math. **37**, 183–186 (American Mathematical Society, Providence, 1980).
[7] P. Slodowy, *Simple Singularities and Simple Algebraic*

Groups, Lecture Notes in Mathematics **815** (Springer-Verlag, Berlin, 1980).

[8] H. Georgi and S. L. Glashow, "Unity of all elementary-particle forces," Phys. Rev. Lett. **32**, 438–441 (1974).

[9] H. Fritzsch and P. Minkowski, "Unified interactions of leptons and hadrons," Ann. Phys. (N.Y.) **93**, 193–266 (1975).

[10] F. Gürsey, P. Ramond, and P. Sikivie, "A universal gauge theory model based on E_6," Phys. Lett. B **60**, 177–180 (1976).

[11] K. Abe, Y. Hayato, T. Iida *et al.* (Super-Kamiokande Collaboration), "Search for proton decay via $p \to e^+\pi^0$ and $p \to \mu^+\pi^0$ in 0.31 megaton·years exposure of the Super-Kamiokande water Cherenkov detector," Phys. Rev. D **95**, 012004 (2017); arXiv:1610.03597.

[12] H. S. M. Coxeter, *Regular Polytopes*, 3rd ed. (Dover Publications, New York, 1973).

[13] J. H. Conway and N. J. A. Sloane, *Sphere Packings, Lattices and Groups*, 3rd ed. (Springer-Verlag, New York, 1999).

[14] R. Slansky, "Group theory for unified model building," Phys. Rep. **79**, 1–128 (1981).

[15] C. Brans and R. H. Dicke, "Mach's principle and a relativistic theory of gravitation," Phys. Rev. **124**, 925–935 (1961).

[16] I. Esteban, M. C. Gonzalez-Garcia, M. Maltoni, T. Schwetz, and A. Zhou, "The fate of hints: updated global analysis of three-flavour neutrino oscillations," J. High Energy Phys. **2020**(09), 178 (2020); arXiv:2007.14792.

[17] R. L. Workman, V. D. Burkert, V. Crede, E. Klempt, U. Thoma *et al.* (Particle Data Group), "Review of Particle Physics," Prog. Theor. Exp. Phys. **2022**, 083C01 (2022).

[18] S. S. McGaugh, F. Lelli, and J. M. Schombert, "Radial Acceleration Relation in rotationally supported galaxies," Phys. Rev. Lett. **117**, 201101 (2016); arXiv:1609.05917.

[19] N. Aghanim, Y. Akrami, M. Ashdown *et al.* (Planck Collaboration), "Planck 2018 results. VI. Cosmological parameters," Astron. Astrophys. **641**, A6 (2020); arXiv:1807.06209.

[20] C. R. Cabrera, L. Tanzi, J. Sanz, B. Naylor, P. Thomas, P. Cheiney, and L. Tarruell, "Quantum liquid droplets in a mixture of Bose–Einstein condensates," Science **359**, 301–304 (2018); arXiv:1708.07806.

[21] G. Gonzalez-Sprinberg and J.-L. Verdier, "Construction géométrique de la correspondance de McKay," Ann. Sci. Éc. Norm. Supér. **16**, 409–449 (1983).

[22] A. D. Sakharov, "Violation of CP invariance, C asymmetry, and baryon asymmetry of the universe," JETP Lett. **5**, 24–27 (1967); [Pis'ma Zh. Eksp. Teor. Fiz. **5**, 32 (1967)].

[23] P. Nath and P. Fileviez Pérez, "Proton stability in grand unified theories, in strings, and in branes," Phys. Rep. **441**, 191–317 (2007); arXiv:hep-ph/0601023.

[24] P. Langacker, "Grand unified theories and proton decay," Phys. Rep. **72**, 185–385 (1981).

[25] J. A. Minahan and D. Nemeschansky, "An N=2 superconformal fixed point with E_6 global symmetry," Nucl. Phys. B **482**, 142–152 (1996); arXiv:hep-th/9608047.

[26] P. Ramond, "The family group in grand unified theories," arXiv:hep-ph/9809459 (1998).

[27] Y. Koide, "New view of quark and lepton mass hierarchy," Phys. Rev. D **28**, 252–254 (1983).

[28] F. An, G. An, Q. An *et al.* (JUNO Collaboration), "JUNO physics and detector," Prog. Part. Nucl. Phys. **123**, 103927 (2022); arXiv:2104.02565.